Isotopically Selective Infrared Multiphoton Dissociation of Vibrationally Excited SiH_4

J. Makowe, O. V. Boyarkin, and T. R. Rizzo*

Laboratoire de Chimie Physique Moléculaire, École Polytechnique Fédérale de Lausanne, CH-1015 Lausanne, Switzerland

Received: December 12, 2001; In Final Form: March 17, 2002

We use mass-resolved 2+2 resonantly enhanced multiphoton ionization (REMPI) of silicon atoms to detect isotopically selective infrared multiphoton dissociation (IRMPD) of both ground-state and vibrationally pre-excited SiH_4. To demonstrate that the detection scheme provides a faithful monitor of the isotopic composition of the primary dissociation products, this approach was first tested on the products generated by both IRMPD and UV photodissociation of phenylsilane. It was then employed to evaluate the degree of isotopic enrichment achieved by IRMPD of ground-state silane using an ammonia laser for dissociation. In a second type of experiment, silane molecules are pre-excited to the first overtone of the Si−H stretch, and then dissociated selectively with the ammonia laser. We find that pre-excitation increases the dissociation cross section by a factor of 230. Tuning the overtone pre-excitation laser while collecting the mass-resolved silicon ion signal generates an overtone excitation spectrum of SiH_4 that is sorted by the silicon isotope. Certain combinations of overtone pre-excitation and ammonia laser dissociation frequencies lead to a high level of isotopic enrichment in the dissociation products: >99% in ^{28}Si or ^{29}Si, and >96% in ^{30}Si. We evaluate the practicality of an overtone-pre-excitation/IRMPD scheme for silicon isotope separation on a macroscopic scale.

I. Introduction

The recent measurement of substantially increased thermal conductivity of silicon[1,2] upon isotopic purification suggests the possibility of using isotopically pure materials to enhance the performance of semiconductor devices. Producing isotopically pure semiconductors is, however, currently limited by the high cost of isotopic enrichment. The development of economically feasible approaches for isotopic enrichment of these materials would facilitate exploring their potential in practical devices. The method of Molecular Laser Isotope Separation (MLIS) using infrared multiphoton dissociation (IRMPD) has shown some promise for laboratory-scale separation of silicon isotopes using Si_2F_6 as a working molecule.[3−6] Starting with a sample of natural isotopic abundance (92.1% ^{28}Si, 4.7% ^{29}Si, and 3.2% ^{30}Si), Kamioka et al.[3] succeeded in enriching SiF_4 dissociation products to 46% in ^{30}Si and 6% in ^{29}Si, while Noda et al.[6] achieved 43.3% and 12.3% for the respective isotopes. Okada et al.[5] reported enrichment of the SiF_2 photoproduct of about 20% for both minor isotopes. While this is currently the most advanced laser-based technique for silicon isotope separation, this level of enrichment is still far below that required for electronic applications.

In a recent publication,[7] we reported the results of a study of IRMPD of SiH_4 using both CO_2 and NH_3 lasers.[8] The use of silane as a parent molecule for isotope separation of Si is attractive, since it is widely employed in the semiconductor industry. Our study revealed that IRMPD of vibrationally ground-state silane is inefficient, exhibiting a laser fluence threshold that is near 17 J/cm^2. In contrast, when the molecules are pre-excited to the first Si−H stretch vibrational overtone before IRMPD, the dissociation is more efficient and exhibits lower threshold fluence. We estimate that vibrational pre-excitation increases the dissociation cross-section by a factor of 230.[7]

These observations suggest potential advantages in using an overtone pre-excitation-IRMPD scheme for silicon isotope separation in SiH_4. In this approach, the pre-excitation laser is tuned to a Si−H stretch overtone transition of silane, promoting primarily a single isotopic species to the upper vibrational level. Following this, a second laser dissociates only the pre-excited molecules via IRMPD, resulting in dissociation products that are substantially enriched in the desired silicon isotope. Implementation of such a scheme for SiH_4 is complicated by the lack of rotational assignments of the first Si−H stretch overtone band of silane. Moreover, our previous investigations revealed that efficient IRMPD of vibrationally pre-excited SiH_4 using a particular line of a NH_3 laser occurs only if the first laser pre-excites the molecules to a particular rotational state.[7] We attribute this selectivity to the requirement that the first few steps of IRMPD be nearly resonant with the frequency of the NH_3 laser when the dissociating fluence is low. The optimal dissociating laser frequencies for particular rotational states of vibrationally pre-excited $^{28}SiH_4$ will not necessarily be the most efficient for other isotopic species, however. To determine the feasibility of this two-laser scheme for enrichment of silicon isotopes, the present work must first assign the rotational transitions of the first Si−H stretch overtone band for the minor Si isotopes. In addition, we must find combinations of overtone pre-excitation frequencies and dissociating frequencies that result in effective, isotopically selective dissociation of $^{29}SiH_4$ and $^{30}SiH_4$.

In our previous study, we used LIF detection of SiH_2 products to monitor the dissociation yield of vibrationally pre-excited silane. Unfortunately, the isotopic shift in the LIF spectra of different Si isotopes of SiH_2 is small and not easily resolved in our experiment, precluding the assignment of the silane Si−H

* Author to whom correspondence should be addressed.

10.1021/jp015609g CCC: $22.00
Published on Web 05/04/2002

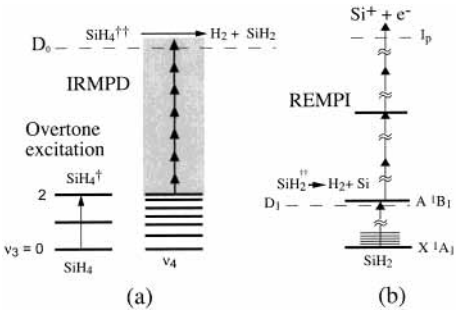

Figure 1. Schematic energy level diagram for (a) IRMPD of vibrationally pre-excited silane, (b) [2+2] REMPI detection of Si atoms in the ^3P or ^1D states. Silicon atoms may appear as a direct product from the IRMPD process or as a result of subsequent photolysis of the IRMPD products (primarily SiH_2) by the ionization laser (see the text).

stretch band for the minor isotopes. In the present work, we overcome this limitation by detecting dissociation products in a mass-resolved manner. We do this by resonance enhanced multiphoton ionization (REMPI) detection of Si atoms in a time-of-flight mass spectrometer (TOF MS). REMPI of silicon atoms in the presence of SiH_4 and its dissociation products has not been thoroughly studied, and there are some contradictions in the literature.[9,10] In the present work we show that REMPI of Si can be used for monitoring relative concentrations of different silicon isotopes in the dissociation products of SiH_4. We then employ this tool to study IRMPD of different isotopic species of vibrationally pre-excited SiH_4 in natural abundance.

II. Experimental Section

Figure 1 shows a schematic energy level diagram for infrared multiphoton dissociation of vibrationally pre-excited SiH_4 combined with REMPI detection of Si. First, an IR laser pulse at approximately 2.3 μm excites the first overtone transition of the Si−H stretch vibration. A few nanoseconds later, a pulse from an NH_3 laser promotes some fraction of the vibrationally excited molecules to energies above the dissociation limit via infrared multiphoton excitation of the ν_4 bending vibration, producing mostly SiH_2. These nascent SiH_2 fragments are subsequently dissociated by a visible laser pulse to produce silicon atoms, and if this third pulse is tuned to a REMPI transition in Si, the latter are ionized by a 2+2 REMPI scheme and detected in a linear time-of-flight mass spectrometer (TOF MS).

We use this scheme to obtain two different types of data. We record mass spectra of silicon atoms from dissociated silane molecules by fixing the frequencies of the excitation, dissociation, and ionization lasers while measuring the time-of-flight of ions corresponding to masses 28, 29, and 30. This allows us to measure the isotopic composition of dissociation products for each particular pair of excitation and dissociation frequencies. In a second type of experiment, we obtain an overtone excitation spectrum of one particular isotopic species of SiH_4 by collecting the ion signal gated at a particular silicon mass as a function of the frequency of the overtone excitation laser while keeping frequencies of the dissociation and probe lasers fixed. Since we monitor the mass signal of one particular Si isotope only, we obtain an isotopically "pure" overtone excitation spectrum. This allows a straightforward assignment of overtone transitions corresponding to different SiH_4 isotopic species.

The experimental apparatus we employ for vibrational overtone excitation and IR MPD of SiH_4 in main has been described elsewhere.[7] To excite the first overtone of the Si−H stretch vibration in SiH_4 (i.e., the $\nu_1+\nu_3$ and $2\nu_3$ bands), we

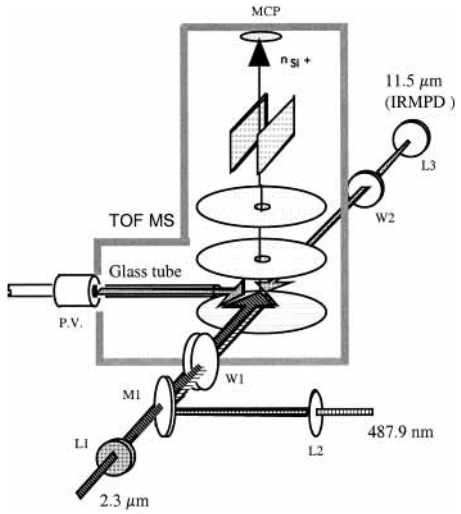

Figure 2. Optical layout of the experiment. The overtone excitation, dissociation, and REMPI (photolysis) laser beams are focused and overlapped with a pulsed molecular jet in the ionization chamber of the TOF MS.

generate 2−4 mJ of infrared radiation around 2.3 μm by difference frequency mixing 100 mJ of the fundamental from a single-mode Nd:YAG laser with the 50 mJ output from a narrow-band (0.03 cm^{-1}) Nd:YAG pumped dye laser. A few nanoseconds later, a microsecond long pulse of 150−250 mJ from an NH_3 laser promotes these pre-excited molecules above the dissociation limit by IRMPD via the H−Si−H bending vibration (ν_4). About 1 μs after the initial laser pulse, a 10 mJ visible pulse from another Nd:YAG pumped dye laser dissociates SiH_2 fragments and subsequently ionizes the resulting Si atoms via a [2+2] REMPI process when tuned to the two-photon $4p^1P_1 \leftarrow 3p^1D_2$ transition at 487.9 nm in atomic silicon. The dissociation of SiH_2 by the visible pulse to form Si atoms in the $^1D_2$ state occurs through excitation of the ground-state silylene fragments to predissociative rovibrational states in the $\tilde{A}$ electronic excited state.[11]

To help clarify the mechanism of SiH_2 dissociation, in some experiments we employ a second ionization dye laser, tuned to 408 nm, to perform [2+1] REMPI of Si through the $4p^3P_0 \leftarrow 3p^3P_0$ transition. In this case, the first ionization laser is detuned from the REMPI resonance to accomplish only the dissociation of SiH_2, while the second one ionizes the silicon atoms. For these diagnostic experiments, we generate SiH_2 fragments either by IRMPD of ground-state silane or by UV photolysis of phenylsilane. In the first case we employ our NH_3 laser for IRMPD, while in the second case we use 10 mJ pulses at 266 nm (4th harmonic of a Nd:YAG laser).

Figure 2 shows the layout of our experiment. The NH_3 laser beam used for IRMPD is focused by an $f = 50$ cm ZnSe lens into the ionization region of a Wiley−McLaren type time-of-flight mass spectrometer (TOF MS), entering through a NaCl window. The IR excitation and UV ionization laser beams are combined on a dichroic mirror (HR at 490 nm, CaF_2 substrate) and enter the chamber through a sapphire window, counter-propagating with the ammonia laser beam. An $f = 50$ cm CaF_2 lens and a $f = 50$ cm fused silica lens focus the IR and 490 nm UV beam, respectively, to a common point between the extraction grids of the mass spectrometer. When the 408 nm UV beam is used for ionization, the focal length of the fused silica lens is reduced to 36 cm to compensate the lower pulse energy at this wavelength and keep the energy fluence at the focus nearly the same.

In previous experiments[7] we have shown that IRMPD of SiH_4 is efficient only when the molecules pre-excited to the first Si−H stretch overtone have rotational quantum numbers in the range $J = 9-13$, depending on the dissociation laser frequency. While these rotational states are well populated at room temperature, their population would be negligible in a typical supersonic molecular beam. To resolve this problem, we have removed the skimmer separating our source chamber and mass spectrometer and introduced a glass tube (Figure 2) of 5 mm internal diameter and 40 mm length. This tube is attached to the pulsed valve and conducts molecules from the nozzle to the dissociation−ionization volume between the accelerating plates of the TOF MS. The effect of this tube is 2-fold: it disrupts the supersonic expansion such that the molecules do not efficiently cool (leaving population in high J states), and it maintains a reasonably high density of molecules in the ionization region. Typical pressures during our experiments are 2×10^{-6} mbar in the ionization region and below 5×10^{-7} mbar at the detector. Having a foreign object between the two electrode plates of the TOF MS unavoidably distorts the homogeneity of the electrical field between them. In our case, this does not affect the mass-resolution of our TOF, but deflects photoions away from the detector. We compensate for this by applying about 300 V on the deflection plates placed in the flight tube of the TOF.

A microchannel plate (MCP) with subnanosecond response time detects the photoions at the end of the 62 cm flight tube. The output signal is first amplified by a 1 GHz preamplifier (EG&G ORTEC, # 9306) and then sent to a 500 MHz digital oscilloscope (LeCroy, LC9350C) which averages the flight-time traces and displays them. The data are transferred to a PC via a GPIB interface for processing. Under the operating conditions employed, we achieve a mass-resolution of about 1000. We have checked the linearity of the detection system by dissociating phenylsilane with a tightly focused ($f = 150$ mm) laser beam of 1 mJ pulse energy at 266 nm and ionizing both the parent molecule and the dissociation products with the same laser pulse. The observed mass spectrum reflects the natural isotopic abundance of Si isotopes. Moreover, variation of the MCP voltage does not change the relative ion signals of the different Si isotopes. This gives us confidence that the detection system remains linear in the dynamical range of our measurements, permitting accurate measurements of isotopic enrichment when we dissociate SiH_4.

We run our experiments at 10 Hz repetition rate, which is determined by that of the NH_3 laser. Each point in an overtone spectrum typically represents an average of 20−30 laser shots; mass spectra are typically averaged over 1000 shots.

III. Results and Discussion

We first report our results on REMPI of Si atoms created by IRMPD or UV photolysis of $PhSiH_3$. This serves to characterize the detection scheme that we subsequently use to study IRMPD of silane. We then present and discuss our results on IRMPD of vibrationally ground-state silane, followed by those on silane molecules that have been pre-excited to the first Si−H stretch overtone before IRMPD.

A. REMPI Detection. With a threshold of ~20 400 cm^{-1}, the lowest energy dissociation channel, $SiH_4 \rightarrow SiH_2 + H_2$, has been shown to dominate in thermal decomposition and in IRMPD of SiH_4[12] under collisional conditions. SiH_2 fragments have also been detected by LIF in our previous study of collision-less IRMPD of silane.[7] Small amounts of other fragments, such as SiH_3,[13] SiH,[14] H_2, and H[15] have been identified in silane decomposition under collisional conditions, and these may also be produced during collisionless IRMPD. Indeed, a strong IR laser field can excite SiH_4 molecules above the lowest dissociation limit, opening the higher energy $SiH_4 \rightarrow SiH_3 + H$ channel at 32 100 cm^{-1}. Moreover, the primary dissociation product, SiH_2, may be further pumped via IRMPD to form Si + H_2 and/or SiH + H. Because different isotopic species of some of these fragments have the same masses (e.g., ^{30}Si and $^{28}SiH_2$), isotopic analysis of the dissociation products, and hence measurements of the degree of isotopic enrichment, is difficult. To overcome this problem, we use REMPI of bare silicon atoms with subsequent detection in a TOF MS. If the detection laser is resonant with an atomic transition of silicon, ionization of Si may predominate over nonresonant ionization of the polyatomic fragments, and the mass spectrum will reflect the silicon isotopic composition (presuming there is no isotopic selectivity in the atomic transition, which is discussed below). If, however, the laser fluence is too high, nonresonant ionization of molecular fragments may become comparable with atomic REMPI and the measured mass spectrum will not reflect the isotopic abundance of the IRMPD products. Thus, our product detection must be performed under conditions (i.e., wavelength and fluence of ionizing radiation) that favor REMPI detection of Si atoms over nonresonant ionization of SiH and SiH_2. As a convenient source of all these fragments we use IRMPD or UV photolysis of phenylsilane. With the available fluence of ammonia laser radiation or 266 nm UV radiation, the dissociation of $PhSiH_3$ is easily saturated, independent of the isotopic species. This ensures that the isotopic composition of the dissociation products reflects the natural abundance of Si. As we show below, this is not the case for SiH_4, where IRMPD of both ground-state and pre-excited silane molecules can be isotopically selective.

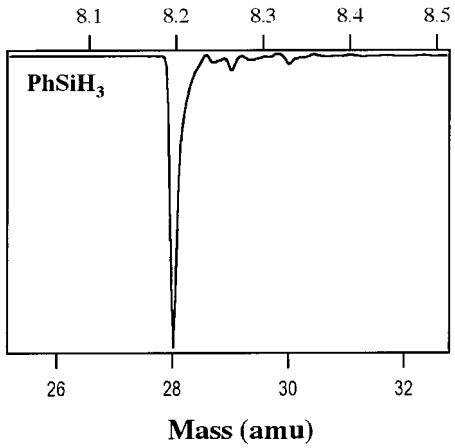

Figure 3. TOF mass spectrum obtained by IRMPD of $PhSiH_3$ with the NH_3 laser tuned to 928 cm^{-1} with [2+2] REMPI of Si at 487.9 nm.

Figure 3 shows a typical REMPI mass spectrum of the IRMPD products of phenylsilane when the ionization laser is tuned to the resonance of Si in the $^1D_2$ state (487.9 nm). Three ion peaks in this spectrum at masses 28−30 correspond to the three Si isotopes. Within the accuracy of our measurements, which is limited by electrical oscillations of the baseline at masses 29 and 30 caused by the strong signal at mass 28, the relative intensities of these peaks reflect the natural abundance of Si. This indicates that we ionize only silicon atoms and that there is no contribution to masses 29 and 30 from $^{28}SiH^+$ and $^{28}SiH_2^+$. The same results have been obtained for several other REMPI transitions and for different ammonia laser lines.

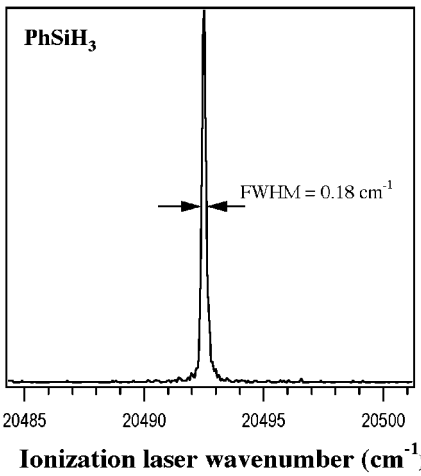

Figure 4. REMPI spectrum of ^{28}Si produced by IRMPD of $PhSiH_3$ by a CO_2 laser tuned to the 10P(32) line (932.89 cm^{-1}). The peak is located at 20492.52 cm^{-1} and is assigned to the $4p^1P_1 \leftarrow 3p^1D_2$ two-photon transition.[27]

We have also performed similar experiments employing UV photolysis of $PhSiH_3$ instead of IRMPD. It is likely that these two dissociation techniques result in different relative distributions of atomic and molecular dissociation products. Changing dissociation channels, however, does not change our results—the ratio of signals at masses 28−30 always corresponds to the natural abundance of Si.

Figure 4 shows the ion signal at mass 28 from UV photolysis of phenylsilane when the ionization laser is tuned through the $4p^1P_1 \leftarrow 3p^1D_2$ REMPI transition around 487.9 nm. The spectrum is obtained at 0.07 cm^{-1} spectral resolution (limited by the scan rate of the laser wavenumber relative to the data collection rate). The ionization laser delivered 1 mJ per pulse in a beam focused by an $f = 50$ cm lens. At this fluence, which is estimated to be about 1−4 J/cm^2, the transition is structureless and exhibits a width of 0.18 cm^{-1} (fwhm). We observe no contribution of power broadening to the line width of this two-photon transition. The same line width is measured if we detected the ion signal at masses 29 and 30 rather than 28. After correction for the instrumental spectral resolution, the residual width of 0.16 cm^{-1} is attributed to Doppler broadening, corresponding to a translational temperature of about 3800 K for the Si dissociation products. As a consistency check, we can compare this value with that determined from the width of the ion time-of-flight peaks. The typical width of a Si^+ peak in our TOF mass spectra is about 10 ns (see, for instance, Figure 3). After deconvoluting the duration (7 ns) and the jitter (2 ns) of the ionization laser pulse, and taking into account the 2 ns resolution of our mass spectrometer, we obtain 6.5 ± 0.5 ns for the duration of the ion pulses. Assuming that this arises from the thermal distribution of Si atoms, we can estimate the temperature by the expression[16]

$$T \cong \frac{(\tau q E_s)^2}{4km} \qquad (1)$$

where τ is the ion pulse duration, $E_s = 10^5$ V/m is the electrical field between the acceleration electrodes, $m = 28$ is the mass of Si, q is the charge, and k is the Boltzmann constant. With $\tau = 6.5 \pm 0.5$ ns, we obtain $T = 4200 \pm 600$ K, consistent with the value obtained from the Doppler width of the silicon REMPI transition. Our observation of relatively sharp REMPI resonances characteristic of atomic transitions in the photodissociation experiments described above confirms that under the conditions employed (i.e., the fluence and frequency of ionization radiation) we detect only Si atoms. This conclusion is consistent with the results of Johannes et al.[17,10] in which they observed no ionized SiH_x ($x = 1-2$) fragments following thermal decomposition of disilane (Si_2H_6). While it is possible that some of the Si atoms that we detect are created by IRMPD of nascent SiH_x ($x = 1-3$) dissociation products, our results indicate that if it does occur, this process is not isotopically selective. Indeed, for all photolysis conditions of $PhSiH_3$, we observe the natural isotopic abundance of the detected Si^+ ions. This fact also demonstrates that the REMPI detection of Si atoms is isotopically nonselective; that is, the measured 0.16 cm^{-1} Doppler width of the REMPI atomic transitions is larger than their isotopic shift. The latter is expected to be in the range of 0.02−0.05 cm^{-1},[18] consistent with our result. Thus, in using this technique to investigate IRMPD of silane, we can be confident that our mass spectra reflect the true isotopic composition of the primary fragments.

To further characterize our REMPI detection scheme for silicon atoms, it is important to identify the mechanism by which these atoms are produced. They may appear as primary dissociation products from IRMPD of SiH_4 or by subsequent dissociation of SiH_x ($x = 2,3$) fragments, either by the IRMPD laser or by the ionization laser radiation used for the REMPI process. Production of Si in the ^1D and ^3P states following photolysis of SiH_2 excited to the $\tilde{A}^1B_1(0, \nu_2\ 0)$ state has been observed by McKay et al.[19] ($Si(^3P)$ for $\nu_2 \geq 2$) and Van Zoeren et al.[11] ($Si(^1D)$ for $\nu_2 \geq 6$). The Si REMPI transition at 488 nm lies within the relatively broad $\tilde{A}^1B_1(060) \leftarrow \tilde{X}^1A_1(0,0,0)$ absorption band of SiH_2, allowing the possibility that the ionization laser pulse excites SiH_2 fragments to the dissociative $\tilde{A}^1B_1$ state. To clarify the source of the Si atoms detected in our experiments, we add a second Nd:YAG pumped dye laser for photolysis of SiH_2 at 488 nm in addition to the REMPI laser. This photolysis laser is detuned from the $Si(^1D)$ REMPI resonance while still overlapping the SiH_2 $\tilde{A}^1B_1(060) \leftarrow \tilde{X}^1A_1(0,0,0)$ absorption band and accomplishes only photolysis of SiH_2. We generate SiH_2 fragments by IRMPD of ground-state SiH_4 using the NH_3 laser. The 488 nm photolysis pulse occurs 550 ns after the beginning of the IRMPD laser pulse and 310 ns before the ionizing laser pulse. The subsequent ionization laser remains tuned to a REMPI transition of Si in the ^3P state (408 nm) or ^1D state (488 nm).

Figure 5 shows three mass spectra obtained after IRMPD of ground-state SiH_4. Trace 5(a) is obtained by Si REMPI at 408 nm with the photolysis laser blocked (2-laser signal). Traces 5(b) and 5(c) are obtained by all three lasers acting together (i.e., the NH_3 laser used for IRMPD, the photolysis laser, and the REMPI laser). In the case of trace 5(b), the photolysis laser is tuned to the $Si(^1D)$ resonance at 487.9 nm; in trace 5(c) it is off-resonance. IRMPD of SiH_4 is accomplished by using the 889 cm^{-1} line of the NH_3 laser in all cases. Note that trace 5(a) shows a weak mass 28 signal due to the ionizing laser at 408 nm, indicating the presence of $Si(^3P)$ atoms produced either by direct IRMPD of SiH_4 or by IRMPD of primary SiH_x ($x = 1-3$) fragments, or by photolysis of SiH_2 by the ionizing laser itself. To our knowledge, SiH_2 transitions at 408 nm have never been observed, although this wavelength is likely to overlap with the $\tilde{A}^1B_1(0,11,0) \leftarrow \tilde{X}^1A_1(0,0,0)$ band. This transition should be relatively weak, because the Franck Condon factor for the transitions with $\nu_2 > 5$ drops significantly.[20] Thus, we believe that SiH_2 photolysis is substantially less efficient at 408 nm than at 487.9 nm. Trace 5(b) shows two mass 28 peaks. The first one is due to the photolysis laser, which is tuned into

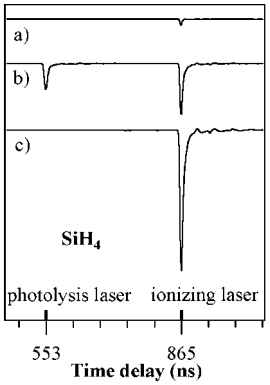

Figure 5. TOF REMPI spectrum of Si(^{3}P) detected at 408 nm, after IRMPD of SiH_4 (NH_3 laser, 889 cm^{-1}) followed by photolysis of dissociation products by radiation near 488 nm: (a) the photolysis beam is blocked, (b) photolysis radiation is tuned to the same $4p^1P_1 \leftarrow 3p^1D_2$ [2+2] REMPI transition in Si as the ionization laser; (c) energy of photolysis laser pulse is increased by 14 times and its frequency is detuned from the REMPI resonance. The ionization laser fires 312 ns after the photolysis laser pulse.

resonance with the Si(^{1}D) REMPI transition at 487.9 nm, and the second peak is due to the ionizing laser at 408 nm. The energy fluence is ~0.5 J/cm^2 for both lasers. The first peak indicates the presence of Si(^{1}D), produced either by IRMPD or by photolysis of SiH_2 by the 487.9 nm ionization laser. The second peak is enhanced by about a factor of 8 with respect to the two-laser signal of trace 5(a), indicating a substantial increase in Si(^{3}P) atoms, which is likely due to the photolysis of SiH_2 by the first laser at 487.9 nm. In trace 5(c), the pulse energy of the photolysis laser is increased by 14 times, and it is tuned out of resonance with the Si(^{1}D) REMPI transition. This causes the first peak to disappear and the Si(^{3}P) signal to increase by ~22 times with respect to trace 5(a). The signal disappears completely when the NH_3 laser beam is blocked. This indicates that a substantial fraction of Si(^{3}P) atoms is produced by the photolysis laser through dissociation of the primary IRMPD products. Under the assumption that photolysis of SiH_2 by the 408 nm REMPI laser is negligible under our experimental conditions, we estimate that at most 4.5% of the primary IRMPD products could be Si(^{3}P) atoms. This result does not change if the photolysis laser wavelength is changed by a few tenths of wavenumbers around the Si REMPI transition at 487.9 nm.

We performed a similar series of experiments by tuning the ionizing laser into resonance with the Si(^{1}D) REMPI transition at 487.9 nm. The results are shown in Figure 6. The three mass spectra are similar to those in Figure 5, except that the ionizing laser probes Si(^{1}D) at 487.9 nm, and IRMPD is performed by the 867.9 cm^{-1} line of the NH_3 laser, which results in an enhancement of the peaks that correspond to the minor Si isotopes (as explained more fully in the following section). The two-laser signal in trace 6(a) shows three peaks, corresponding to the three Si isotopes in the ^{1}D state, produced either by IRMPD of SiH_4 and/or by photolysis of SiH_2 by the ionizing laser itself. The first three peaks in trace 6(b) originate from both dissociation and ionization of silicon isotopes by the photolysis laser, which is tuned into resonance with the Si(^{1}D) REMPI transition at 487.9 nm. The second set of peaks correspond to isotopes of Si(^{1}D) ionized by the second (ionizing) laser. Although the fluence of the ionizing laser is the same as that in trace 6(a), the corresponding signal in trace 6(b) is about 10% less, indicating that the concentration of Si(^{1}D) atoms is depleted by the photolysis laser. Trace 6(c) demonstrates that when the photolysis laser is tuned off the Si(^{1}D) resonance, the

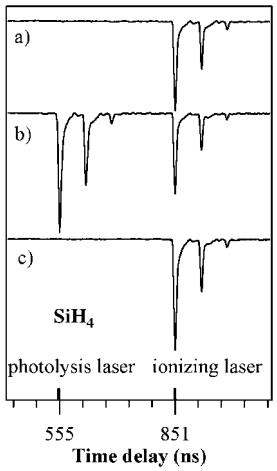

Figure 6. TOF REMPI spectrum of Si(^{1}D) detected at 487.9 nm, after IRMPD of SiH_4 (NH_3 laser, 867.9 cm^{-1}) followed by photolysis of dissociation products by 488 nm radiation: (a) the photolysis beam is blocked; (b) the photolysis laser is tuned to the same wavelength as the ionization laser; (c) photolysis laser is tuned off the REMPI resonance while its pulsed energy remains the same in all three experiments. The ionization laser fires 296 ns after the photolysis laser.

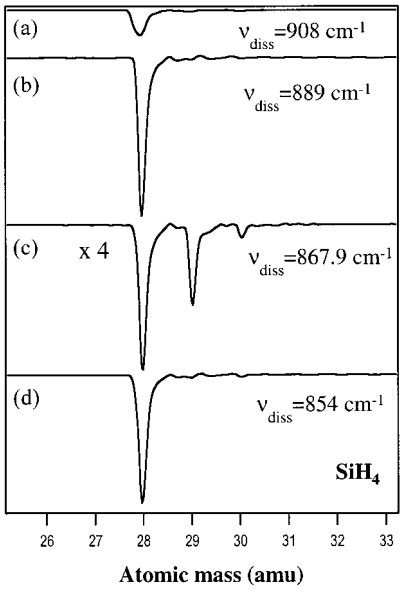

Figure 7. TOF mass spectra of fragments created by IRMPD of ground-state SiH_4, detected by REMPI of Si(^{1}D) at 487.9 nm. The spectra are labeled by the wavenumber of dissociating radiation (NH_3 laser). The relative intensities of the traces are shown as they appear in the experiment, except for the trace with $n_{diss} = 867.9$ cm^{-1}, which is magnified by a factor of 4.

earlier set of peaks vanishes and the latter increase by about 25%. Taken together with the data of Figure 5, these data clearly indicate that the photolysis of primary IRMPD dissociation fragments by the ionization radiation is an important source of Si atoms in both the ^{3}P and ^{1}D electronic states.

Having characterized our REMPI detection scheme and determined parameters of the ionization radiation that allows unbiased detection of all three Si isotopes, we now describe experiments where this detection tool is employed to study isotopic selectivity in the IRMPD of silane.

B. IRMPD of Ground-State Silane. Figure 7 shows ion signals at masses 28−30 detected by REMPI of Si at 487.9 nm after IRMPD of SiH_4 using different lines of the NH_3 laser. The experimental conditions are the same in each case except

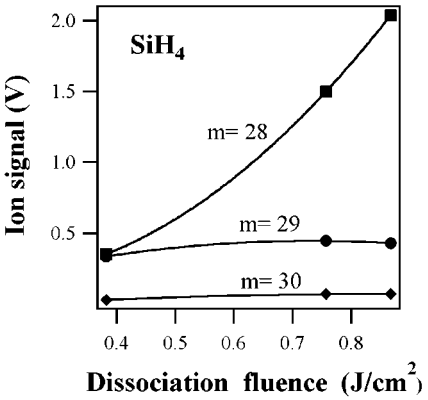

Figure 8. Relative intensities of TOF REMPI signals of Si(^{1}D) at masses 28−30 as a function of fluence of the NH_3 dissociation laser tuned to the 867.9 cm^{-1} line.

for the different power available at the various ammonia laser frequencies. Because the IRMPD process is nonlinear, we do not normalize the spectra to the ammonia laser power. All the spectra clearly show the most intense feature at mass 28, corresponding to IRMPD of the main isotopic species $^{28}SiH_4$, and smaller signals at masses 29, 30, corresponding to the minor isotopic species. The 854 and 889 cm^{-1} lines of ammonia laser (i.e., traces 7(b) and 7(d), respectively) appear to be the most efficient for dissociating ground-state $^{28}SiH_4$. The relative intensities of ion signals at masses 28−30 after dissociation with these laser lines are close to the natural abundance of Si. This is not the case for certain other dissociation lines, however. The most prominent example of enrichment of the products in the minor isotopes is shown in Figure 7(c), where the dissociation ammonia laser is tuned to the line at 867.9 cm^{-1}. The relative signals at masses 28 and 29 imply that dissociation products are enriched to about 35% in the latter. As shown in Figure 8, this degree of enrichment increases further as the fluence of the 867.9 cm^{-1} dissociating radiation is lowered. Although the signal at mass 28 increases with fluence, the signals at masses 29 and 30 remain about the same over the fluence range investigated. Such dependence suggests that dissociation of $^{29}SiH_4$ and $^{30}SiH_4$ is already saturated at a fluence as low as 0.4 J/cm^2, at which point the concentration of ^{29}Si the in dissociation products reaches 47%—a 10-fold increase over its natural abundance.

Isotopic selectivity in IRMPD of polyatomic molecules is not new, having been first demonstrated in the mid 1970s.[21−24] However, silane is different from typical working molecules for laser isotope separation by IRMPD. Usually one chooses a parent molecule possessing a vibrational mode with an isotopic shift that is at least comparable to the width of the room temperature rotational contour. To achieve isotopic selectivity and efficient dissociation, the dissociation laser is tuned to the low frequency side of the absorption band of the ground state molecules. Selectivity is gained over several absorption steps during the IRMPD process. The rotational identity of the first absorption step and the exact frequency of dissociation radiation are usually not critical. In contrast, the isotopic shift in SiH_4 is rather small (∼1.3 and 2.6 cm^{-1} [25] for $^{29}SiH_4$ and $^{30}SiH_4$, respectively), and thus the ν_4 absorption bands of the three isotopes are largely overlapped. Moreover, the high average frequency of the vibrational modes in SiH_4 leads to a low density of vibrational states in the energy region of the first few steps of IRMPD, and the large rotational constant leads to a sparse rotational structure—both of which make collision-free IRMPD of ground-state SiH_4 difficult. However, if the dissociation frequency is in close resonance with a particular rotational transition of the desired isotopic species, molecules in this state may be dissociated with only moderate laser fluence. In our previous work,[7] we observed such rotational selectivity for IRMPD of vibrationally pre-excited molecules, and one expects a similar degree of selectivity for IRMPD of ground-state silane. The 867.9 cm^{-1} ammonia laser line is in close resonance with one of the components of the split P(13) rotational transition in $^{29}SiH_4$,[25] favoring dissociation of this species. In light of this, the data of Figure 8 suggest that absorption from only one particular rotational state of $^{29}SiH_4$ is saturated. In other words, although the IRMPD is saturated, only a small fraction of all irradiated molecules is dissociated. Indeed, in SiH_4, each single J level is split by Coriolis interaction to several sublevels. A strong Coriolis coupling between the ν_4 and the ν_2 modes causes this splitting to become significant for the high J states of the ν_4 vibration that we use for multiphoton pumping, and it increases upon vibrational excitation. At moderate fluence, after a few excitation steps, the narrow bandwidth dissociation radiation of our multimode NH_3 laser (typically 0.1 cm^{-1}) may overlap with only a few of the many possible components of the transition to the next higher vibrational level. Therefore, some of the excited molecules will remain in low-lying levels and will never reach the dissociation threshold. At high fluence, power broadening may result in opening new excitation pathways, increasing the overall dissociation yield, although the isotopic selectivity may decrease. Thus, even though IRMPD of ground state silane is isotopically selective, it is difficult to implement this process for practical isotope separation because of the low overall dissociation yield. This problem can potentially be overcome by overtone pre-excitation of molecules directly to a high vibrational energy level, jumping over the bottlenecks in the IRMPD process. One also expects that isotopic selectivity in such approach can be higher, since it is mainly determined by the pre-excitation step. The following subsection presents our results on IRMPD of different isotopes of SiH_4 pre-excited to the first Si−H stretch overtone.

C. IRMPD of Vibrationally Pre-excited Silane. The isotopic shift of the Si−H stretch fundamental has been estimated to be −1.4 cm^{-1} for $^{29}SiH_4$ and −2.9 cm^{-1} for $^{30}SiH_4$,[25] and the corresponding shifts for the first Si−H stretch overtone should be nearly twice these values. To our knowledge, rotationally resolved spectra of the first overtone of the Si−H stretch vibration in $^{29}SiH_4$ and $^{30}SiH_4$ have never been assigned. Thus, our primary objective is to find and to assign transitions in the excitation spectrum of the first Si−H stretch overtone silane corresponding to the minor silicon isotopes.

Figure 9(a)−(d) presents four excitation spectra in the first Si−H stretch overtone band of SiH_4 in natural isotopic abundance. Each of these spectra is obtained using the IRLAPS technique, but the dissociation fragments are detected differently. In 9(a) we use laser-induced fluorescence of SiH_2, which is not isotopically selective, while in 9(b)−(d) we use REMPI of Si followed by mass spectrometric detection of the resulting silicon ions. For comparison, we also show in Figure 9(e) a photoacoustic spectrum of silane over the same spectral region.

By monitoring the ion signal at a particular silicon mass while scanning the frequency of the overtone excitation laser, we obtain an excitation spectrum of a single isotopic species of silane. Comparison of the isotopically selective "action" spectra with the photoacoustic spectrum allows assignment of some of the absorption features in the latter to transitions of the different isotopic species. Some of these transitions are isotopically "pure" in the sense that they primarily belong to a single isotopic

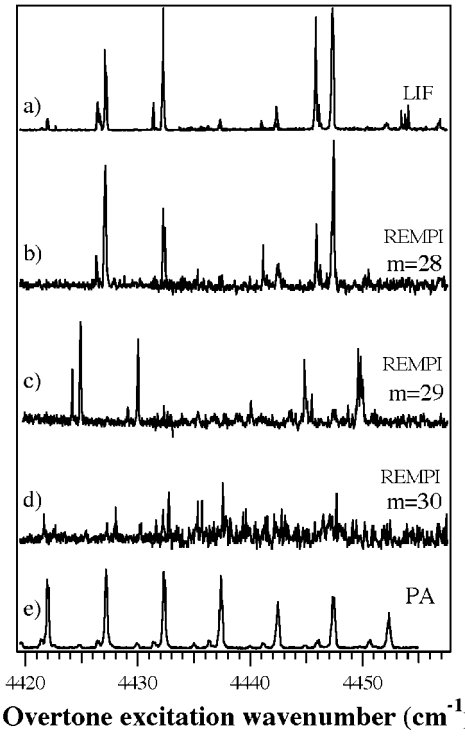

Figure 9. (a−d) A part of the action spectra of the first Si−H stretch overtone in SiH_4 obtained using our IRLAPS[28] detection technique: (a) with LIF detection of SiH_2 fragments[7] and (b), (c), (d) with mass-resolved TOF REMPI detection of ^{28}Si, ^{29}Si, and ^{30}Si isotopic species (^1D state), respectively. For comparison, trace (e) shows a photoacoustic spectrum of the same transition.

species. Pre-excitation of silane through these transitions produces vibrationally excited SiH_4 molecules that are highly enriched in a single isotope of Si. If one performs selective IRMPD of these molecules, the dissociation products will be enriched in one of the Si isotopes.

As observed in our previous work, efficient IRMPD of silane from the first Si−H stretch overtone level occurs only when molecules are pre-excited to certain rotational states that depend on the frequency of the dissociation laser. This rotational selectivity arises from the need for the dissociating radiation to maintain a close resonance with rovibrational transitions for the first few steps of multiphoton excitation. Isotopically selective detection of Si fragment reveals that in addition to the rotational selectivity, IRMPD of the pre-excited molecules is isotopically selective—that is, each particular line of the ammonia laser favors dissociation of a particular pre-excited isotopic species from a few specific rotational states (Figure 9(b),(c)). We believe that the mechanism of the isotopic selectivity in IRMPD of pre-excited silane is exactly the same as the mechanism of the rotational selectivity, arising from a slight difference in the frequency of the ν_4 transition for different pre-excited isotopic species.

Figure 10 shows an example of Si ion time-of-flight traces in the mass-range 28−30 from the IRMPD of silane molecules that have been vibrationally pre-excited to the first Si−H stretch overtone. Trace 10(a) shows the signal when the overtone pre-excitation laser is blocked, while 10(b) shows the result of tuning the overtone excitation laser to a strong isotopically "pure" transition of $^{29}SiH_4$ at 4425.03 cm^{-1}. Trace 10(c) is simply the difference of (b) and (a). In each case, the ammonia laser has been tuned to a line at 867.9 cm^{-1}. When the pre-excitation laser is blocked, the ion signal originates from IRMPD of the ground-state silane. As was discussed above, this process shows

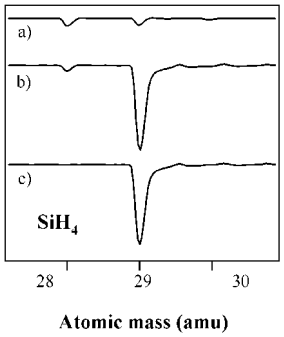

Figure 10. TOF REMPI mass-spectra of Si(^1D) in dissociation products of SiH_4 resulting from (a) IRMPD of ground-state silane, (b) IRMPD of SiH_4 pre-excited at 4425.03 cm^{-1}. Trace (c) is a result of subtraction of trace (a) from trace (b). The dissociating NH_3 laser is tuned to the 867.9 cm^{-1} line.

some degree of isotopic selectivity, and hence the mass spectrum in Figure 10(a) does not reflect the natural abundance of Si. When the excitation laser is unblocked, the signal at mass 29 rises significantly relative to that at mass 28, indicating that pre-excitation of $^{29}SiH_4$ increases both the IRMPD efficiency as well as the overall isotopic selectivity of the process. The relative intensities of the peaks in trace 10(b) imply an isotopic abundance of ^{29}Si in the dissociation products of 93%. The degree of isotopic enrichment is limited by three factors.

The first is IRMPD of ground-state silane, which produces a background of the other isotopes. Although this process is itself isotopically selective, the selectivity is not nearly as high as the two-laser processes and it is not necessarily selective for the same isotope. The second limiting factor is the low fraction of $^{29}SiH_4$ pre-excited to the first overtone level. This fraction, which determines the intensity of the mass-29 signal in the trace on Figure 10(b), is proportional to the pre-excitation laser fluence. By decreasing the fluence of the dissociating laser and/or increasing the fluence of the pre-excitation laser, the relative intensity of the background signal can be suppressed and consequently the isotopic purity of dissociation products substantially increased. Figure 10(c), which shows the difference between traces (b) and (a), represents the hypothetical limit for the selectivity of this particular excitation scheme. This limit is determined by the spectroscopic purity of the excited overtone transition and depends on the frequency and line width of the pre-excitation laser.

We have explored different combinations of pre-excitation and dissociation frequencies for isotopically selective IRMPD of the three isotopic species of SiH_4. Table 1 summarizes the most selective of these combinations. The example discussed above for ^{29}Si, which uses pre-excitation at 4425.03 cm^{-1} and dissociation at 867.9 cm^{-1}, gives the highest measured dissociation yield and at the same time allows enrichment of the dissociation products to >99% in the minor isotope. The same level of enrichment can be reached for ^{28}Si if 4377.62 and 854 cm^{-1} are employed for pre-excitation and IRMPD, respectively. For ^{30}Si, the maximum possible enrichment does not exceed 96%.

In addition to high isotopic selectivity, the absolute yield is an important characteristic of any isotope separation process, since it is central in determining the cost. Our estimate shows that with the 3−5 mJ pulse energy available from our overtone excitation laser, we excite no more than 1% of molecules of a desired isotopic species to the required rovibrational level at the laser beam waist. Moreover, to preserve high selectivity, the dissociating fluence should be sufficiently low, resulting in dissociation of only half of the pre-excited molecules. We

TABLE 1: Summary of the Results on Isotopically Selective IRMPD of Pre-excited SiH_4[a]

mass (amu)	excitation wavenumber (cm^{-1})	relative intensity	maximum enrichment (%)	experimental enrichment (%)
28	4244.84	0.31	>99	>96
	4307.59	0.41	>98	>96
	4356.66	1	>98	>97
	4364.61	0.39	>98	>97
	4427.44	0.86	>99	>98
29	4309.85	0.36	>97	>80
	4355.88	0.76	92	85
	4425.03	1	>99	>93
30	4247.00	0.19	33	19
	4250.97	0.23	76	20
	4304.05	1	56	52
	4348.07	0.33	>96	>35

[a] The dissociating NH_3 laser is tuned to the 867.9 cm^{-1} line. Only strong overtone transitions are shown. The absolute dissociation yield is about 10 and 24 times lower, respectively, for ^{29}Si and ^{30}Si compared with ^{28}Si. Maximum enrichment represents an upper limit for the level of isotopic enrichment, determined by spectral overlap of transitions of different isotopic species in naturally abundant SiH_4. Experimental enrichment is the level of isotopic enrichment observed in our experiments.

therefore expect a total yield on the order of 0.5%. For the process to be performed under collision-free conditions, the sample pressure should not exceed 1−2 mbar. This results in an overall absolute yield on the order of 10^{10} molecules/mm^3 per laser shot. The volume near the focus, where efficient pre-excitation and dissociation take place under our conditions, is a few tens of mm^3. Therefore, we produce not more than 10^{-8} grams of ^{29}Si per hour at more than 90% isotopic purity. This productivity is too low for practical applications.

The two primary factors that limit the productivity of this process are the low power of our pre-excitation laser and the small fraction of molecules available for excitation. The latter has two components. Only molecules in a single rotational state may be pre-excited via a chosen transition, and for $J = 8-12$, the fraction of molecules in these states is only 5−10% at room temperature. Moreover, the requirement for the process to be collisionless limits the maximum sample pressure and therefore the total number of available molecules. It is not clear whether the process must occur in a collisionless environment, however. On one hand, collisions may allow fast rotational relaxation during the pre-excitation pulse and hence refill the rotational state depopulated by overtone excitation, resulting in higher pre-excitation efficiency. On the other hand, v−v collisional energy transfer may scramble the isotopic purity of excited molecules. However, as it has been recently demonstrated in our laboratory,[26] under certain conditions collisional v−v relaxation may preserve and even enhance isotopic selectivity. The mechanism of this enhancement is not yet fully understood, and, therefore, it is not clear if it can be extended to IRMPD of vibrationally pre-excited SiH_4.

IV. Conclusions

Laser radiation at 487.9 nm at a fluence up to 1 J/cm^2 allows [2+2] REMPI detection of Si via the $4p^1P_1 \leftarrow 3p^1D_2$ 2-photon transition without noticeable ionization of SiH_x ($x = 1-3$) fragments created by IRMPD of silane. This allows the use of REMPI for monitoring the isotopic composition of the IRMPD dissociation products. A substantial fraction of the detected Si atoms is created through photolysis of nascent SiH_x ($x = 1-3$) fragments by the ionization laser.

Infrared multiphoton dissociation of vibrationally ground-state SiH_4 by certain lines of an ammonia laser exhibits isotopic selectivity. The dissociation products can be enriched in either of the two minor silicon isotopes, ^{29}Si or ^{30}Si, depending on frequency of the dissociating laser. For example, IRMPD of vibrationally ground-state SiH_4 by 867.9 cm^{-1} radiation results in more than 10-fold enrichment of dissociation products in ^{29}Si. However, the low density of vibrational levels for the first several steps of IR MPD makes such isotopically selective dissociation inefficient.

Both the isotopic selectivity and dissociation yield can be greatly increased if SiH_4 molecules are pre-excited to the first Si−H stretch overtone level followed by IRMPD of the pre-excited species. High enrichment of SiH_4 dissociation products in a particular Si isotopic species requires certain combinations of the pre-excitation and the dissociation frequencies (Table 1). The pre-excitation frequency is optimized for high isotopic selectivity, while the dissociation frequency is optimized for maximum dissociation yield from the prepared excited rovibrational state of a given isotopic species. At high fluence of the pre-excitation laser, the dissociation products could in principle be enriched up to 99% in ^{29}Si or up to 96% in ^{30}Si. Although much higher than the yield of isotopically selective IRMPD of ground-state silane, the overall yield of the overtone pre-excitation-IRMPD process is still too low for a practical implementation of this approach to isotope separation of silicon with SiH_4 as a parent molecule. This yield is limited by low sample pressure and by the small fraction of molecules in single rotational states suitable for excitation. Nevertheless, as we have demonstrated in this work, the suggested overtone pre-excitation-IRMPD approach has potential for highly selective molecular isotope separation. If low overtone transitions of the parent molecule can be rotationally resolved, a high degree of isotopic selectivity can be reached in a single-stage process, even if the isotopic shift is too small to perform classical, isotopically selective IRMPD. The productivity of the process could be increased by selection of parent molecules with suitable spectroscopy, by controlling the rotational temperature of the molecules and by improving the tunability of the dissociation laser.

Acknowledgment. This work has been supported by the École Polytechnique Fédérale de Lausanne (EPFL) and the Swiss National Foundation through Grant 20-59261.99.

References and Notes

(1) Capinski, W. S.; Maris, H. J.; Bauser, E.; Silier, I.; Asenpalmer, M.; Ruf, T.; Cardona, M.; Gmelin, E. *Appl. Phys. Lett.* **1997**, *71*, 2109−2111.

(2) Ruf, T.; Henn, R. W.; Asen-Palmer, M.; Gmelin, E.; Cardona, M.; Pohl, H. J.; Devyatych, G. G.; Sennikov, P. G. *Solid State Commun.* **2000**, *115*, 243−247.

(3) Kamioka, M.; Arai, S.; Ishikawa, Y.; Isomura, S.; Takamiya, N. *Chem. Phys. Lett.* **1985**, *119*, 357−360.

(4) Tanaka, K.; Sh., I.; Kaetsu, H.; Yatsurugi, Y.; Hashimoto, M.; Togashi, K.; Arai, S. *Bull. Chem. Soc. Jpn.* **1996**, *69*, 493−498.

(5) Okada, Y.; Takeuchi, K. *J. Nucl. Sci. Technol.* **1997**, *34*, 413−415.

(6) Noda, T.; Suzuki, H.; Araki, H. *Fusion Eng. Des.* **1998**, *41*, 173−179.

(7) Makowe, J.; Boyarkin, O. V.; Rizzo, T. R. *J. Phys. Chem. A* **2000**, *104*, 11505−11511.

(8) Makowe, J.; Boyarkin, O. V.; Rizzo, T. R. *Rev. Sci. Instrum.* **1998**, *69*, 4041−4043.

(9) Robertson, R. M.; Rossi, M. J. *Appl. Phys. Lett.* **1989**, *54*, 185−187.

(10) Johannes, J. E.; Ekerdt, J. G. *J. Appl. Phys.* **1994**, *76*, 3144−3148.

(11) Van Zoeren, C. M.; Thoman, J. W.; Steinfeld, J. I.; Rainbird, M. W. *J. Phys. Chem.* **1988**, *92*, 9−11.

(12) Mick, H. J.; Roth, P.; Smirnov, V. N. *Kinet. Catal. (Engl. Trans.)* **1994**, *35*, 764−767.
(13) Borsella, E.; Caneve, L. *Appl. Phys. B* **1988**, *46*, 347−355.
(14) Schmitt, J. P. M.; Gressier, P.; Krishnan, M.; de Rosny, G.; Perrin, J. *Chem. Phys.* **1984**, *84*, 281−293.
(15) Deutsch, T. F. *J. Chem. Phys.* **1979**, *70*, 1187−1192.
(16) Wiley, W. C.; McLaren, I. H. *Rev. Sci. Instrum.* **1955**, *26*, 1150−1157.
(17) Johannes, J. E.; Ekerdt, J. G. *J. Electrochem. Soc.* **1994**, *141*, 2135−2140.
(18) Babichev, A. P.; Babyshkina, N. A.; Bratkovskii, A. M.; Brodov, M. E.; et al. *Physical values: reference book*; Energoatomizdat: Moscow, 1991.
(19) McKay, R. I.; Uichanco, A. S.; Bradley, A. J.; Holdsworth, J. R.; Francisco, J. F.; Steinfeld, J. I.; Knight, A. E. W. *J. Chem. Phys.* **1991**, *95*, 1688−1695.
(20) Fukushima, M.; Mayama, S.; Obi, K. *J. Chem. Phys.* **1992**, *96*, 44−52.
(21) Ambartsumyan, R. V.; Letokhov, V. S.; Ryabov, E. A.; Chekalin, N. V. *JETP Lett.* **1974**, *20*, 273.
(22) Ambartsumyan, R. V.; Gorokhov, A. Y.; Letokhov, V. S.; Makarov, G. N. *JETP Lett.* **1975**, *21*, 171.
(23) Ambartsumyan, R. V.; Gorokhov, A. Y.; Letokhov, V. S.; Makarov, G. N.; Puretskii, A. A. *JETP Lett.* **1976**, *23*, 22.
(24) Lyman, J. L.; Rockwood, S. D. *J. Appl. Phys.* **1976**, *47*, 595−601.
(25) Johns, J. W. C.; Kreiner, W. A.; Susskind, J. *J. Mol. Spectrosc.* **1976**, *60*, 400−411.
(26) Kowalczyk, M.; Boyarkin, O. V.; Rizzo, T. R. Highly selective laser isotope separation of 13-C. To be published.
(27) Ioannidou-Philis, A.; Philis, J. G.; Christodoulides, A. A. *J. Mol. Spectrosc.* **1987**, *121*, 50−60.
(28) Boyarkin, O. V.; Settle, R. D. F.; Rizzo, T. R. *Ber. Bunsen-Ges. Phys. Chem.* **1995**, *99*, 504.